

University of Groningen

New imaging strategies in neuroendocrine tumors

van Asselt, Sophie

DOI:
[10.1016/j.gie.2014.09.037](https://doi.org/10.1016/j.gie.2014.09.037)

IMPORTANT NOTE: You are advised to consult the publisher's version (publisher's PDF) if you wish to cite from it. Please check the document version below.

Document Version
Publisher's PDF, also known as Version of record

Publication date:
2014

[Link to publication in University of Groningen/UMCG research database](#)

Citation for published version (APA):
van Asselt, S. (2014). *New imaging strategies in neuroendocrine tumors*. [s.n.].
<https://doi.org/10.1016/j.gie.2014.09.037>

Copyright

Other than for strictly personal use, it is not permitted to download or to forward/distribute the text or part of it without the consent of the author(s) and/or copyright holder(s), unless the work is under an open content license (like Creative Commons).

Take-down policy

If you believe that this document breaches copyright please contact us providing details, and we will remove access to the work immediately and investigate your claim.

Downloaded from the University of Groningen/UMCG research database (Pure): <http://www.rug.nl/research/portal>. For technical reasons the number of authors shown on this cover page is limited to 10 maximum.

Chapter 3

Endoscopic ultrasound is superior compared to standard imaging for detection of pancreatic solid lesions in von Hippel-Lindau patients

Sophie J. van Asselt

Adrienne H. Brouwers*

Hendrik M. van Dullemen*

Eric J. van der Jagt

Alfons H.H. Bongaerts

Klaas P. Koopmans

Ido P. Kema

Bernard A. Zonnenberg

Henri J.L.M. Timmers

Wouter W. de Herder

Wim J. Sluiter

Elisabeth G.E. de Vries

Thera P. Links

*Those authors contributed equally and are both second author

Submitted

Abstract

Background Patients with von Hippel-Lindau (VHL) disease are prone to develop pancreatic neuroendocrine tumors (pNETs). However, the best imaging technique for detection of pNETs in VHL is currently unknown.

Aim In a head-to-head comparison we evaluated endoscopic ultrasound (EUS) and ¹¹C-5-hydroxytryptophan positron emission tomography (¹¹C-5-HTP PET) relative to standard screening for pancreatic solid lesion detection.

Design We conducted a cross-sectional study in 22 patients at a tertiary care university medical center. Patients with a VHL mutation or with one VHL manifestation and a mutation carrier as 1st grade family member, with recent screening by abdominal computed tomography (CT) or magnetic resonance imaging (MRI) and somatostatin receptor scintigraphy (SRS), were eligible. Patients underwent linear EUS combined with power Doppler and ¹¹C-5-HTP PET. Patient and lesion-based positivity for pancreatic solid lesions were calculated for all imaging techniques with a composite reference standard.

Results In 10 of the 22 patients, 20 pancreatic solid lesions were detected: 17 with EUS ($P < .05$ versus CT/MRI+ SRS), 3 with ¹¹C-5-HTP PET, 3 with SRS, 9 with CT/MRI and 9 with CT/MRI+ SRS. With EUS, the solid lesions had a median size of 9.7 mm (range 2.9-55 mm) and most were homogeneous, hypoechoic, iso-elastic and hypervascular. Moreover, EUS detected multiple pancreatic cysts in 18 patients with a median of 4 cysts (range 1-30) per patient.

Conclusions EUS is superior to CT/MRI+ SRS for detecting pancreatic solid lesions in VHL disease. ¹¹C-5-HTP PET has no value.

Introduction

Pancreatic neuroendocrine tumors (pNETs) are uncommon neoplasms with an incidence of 1-10 per 1 million in the general population.^{1,2} pNETs can occur sporadically or as part of the hereditary multiple tumor syndromes von Hippel-Lindau (VHL) disease and Multiple Endocrine Neoplasia type 1. VHL disease is a dominantly inherited multiple tumor syndrome that results from a germline mutation in the *VHL* gene, located on chromosome 3 (3p25-26).³ The incidence is 1 per 36,000 live births.⁴ VHL disease can lead to the development of benign and malignant tumors in various organ systems, including hemangioblastomas in the central nervous system, renal cysts and clear cell renal cell carcinomas, pheochromocytomas, pancreatic cysts and pNETs. VHL patients have a shorter life expectancy compared to the general population, and 73% of deaths are VHL disease-related.⁵ Therefore, VHL patients undergo screening to detect manifestations at an early stage.⁶

Non-functional pNETs are present in 10-17% of the VHL patients.⁷⁻⁹ In addition, 71% of the VHL patients have pancreatic cysts including serous microcystic cystadenomas, which are benign lesions that rarely require intervention.⁷ Since the only curative treatment for pNETs is surgery, timely detection is critical. Surgery should be considered based on one of the following: germline mutation in the *VHL* gene located on exon 3, tumor doubling rate < 500 days and/or tumor size > 3 cm.^{8,10} For screening of the kidneys, adrenals and pancreas yearly abdominal computed tomography (CT) is recommended from 18 years of age.⁶ The VHL handbook, revised in 2012, recommends high-quality abdominal ultrasound yearly and magnetic resonance imaging (MRI) at least every other year from 16 years of age onwards.¹⁰ In case of suspicion of a sporadic pNET, the National Comprehensive Cancer Network (NCCN) guideline recommends multiphase CT or MRI, and suggests that somatostatin receptor scintigraphy (SRS) plus circulating tumor markers (serum chromogranin A and plasma pancreatic polypeptide) can be considered.¹¹

Currently, the best imaging technique for early detection of pNETs in VHL disease is unknown. Moreover, differentiation between serous microcystic cystadenomas and pNETs on radiological imaging can be difficult.^{6, 8-9, 12} In 69 VHL patients with pancreatic solid lesions, abdominal CT was more sensitive for detection of pancreatic lesions than MRI, 6-[F-18]fluoro-L-dihydroxyphenylalanin (¹⁸F-DOPA) and ¹⁸F-fluorodeoxyglucose (¹⁸F-FDG) positron emission tomography (PET).¹² The disadvantage of CT, however, is its radiation burden, which may be even more undesirable in genetically vulnerable VHL patients.

Two new imaging strategies are available for detection of pNETs: endoscopic ultrasound (EUS) and ^{11}C -5-hydroxytryptophan (^{11}C -5-HTP) PET. In a retrospective control study in patients without a hereditary multiple tumor syndrome, EUS identified 82% of histological proven functional pNETs, undetectable by trans-abdominal ultrasound and CT.¹³ No such studies are available in VHL patients. ^{11}C -5-HTP is a precursor of serotonin which neuroendocrine cells can take up, decarboxylate into ^{11}C -serotonin and store in vesicles.¹⁴ A PET scan with this tracer could potentially provide insight into the neuroendocrine nature of a pancreatic lesion. ^{11}C -5-HTP PET was more sensitive to detect lesions in patients with advanced pNETs than SRS and ^{18}F -DOPA PET.¹⁵ The aim of this study was therefore to evaluate EUS and ^{11}C -5-HTP PET in a head-to-head comparison relative to standard screening for the detection of pNETs in VHL patients.

Patients and methods

Patients

In this prospective study, patients under standard surveillance in the VHL centers of the Erasmus MC Rotterdam, University Medical Centers Utrecht and Groningen were referred to the University Medical Center Groningen for study participation. Patients were included between February 2009 and August 2011. Eligible were patients with a VHL mutation or with one VHL-manifestation and a mutation carrier as 1st grade family member, with an age of ≥ 18 years. Excluded were pregnant patients or patients with known alcohol abuse and/or chronic pancreatitis. The study was approved by the Medical Ethics Committee of Groningen, and all patients gave written informed consent. The study was registered at the Dutch trial registry under <http://www.trialregister.nl/trialreg/index.asp> (NTR1668).

Before study entry, standard work-up screening had to be performed in the patient's own center, consisting of SRS within 6 months, and abdominal CT or MRI and serum/plasma tumor markers within 4 months. With radio-immunoassays, serum levels of chromogranin A (CgA-React, Cis Bio International, Gif-sur-Yvette, France, upper limit of normal 100 $\mu\text{g}/\text{L}$) and plasma levels of pancreatic polypeptide (Eurodiagnostica, Nijmegen, the Netherlands, upper limit of normal 100 pmol/L) were determined. Since the use of proton pump inhibitors can lead to spurious elevation of chromogranin A,¹⁶ patients on proton pump inhibitors were excluded from analysis of these levels. Values $>$ upper limit of normal were considered as overproduction.

CT/MRI

Patients underwent abdominal CT or MRI, depending on the preference of the treating physician. CT scans were performed with a multidetector CT scanner, before and after intravenous (IV) administration of iodine-containing contrast agent. MRI scans were performed in T1 and T2-weighted sequences, with and without IV administration of gadolinium-containing contrast agent.

The reconstruction interval varied between 0.75 and 5.0 mm. Lesions were recorded as pancreatic solid lesions when they were hyperattenuating lesions on contrast images during the arterial or portal venous phase. On MRI, lesions with low intensity on T1 sequences and high intensity on T2 sequences compared to pancreatic tissue were considered as solid.¹⁷ CT and MRI scans were reviewed by a radiologist (EJvdJ) blinded for clinical information. In case of discrepancy between the radiologist of the referral and research center, a second radiologist (AHHB) reviewed these particular scans and consensus between EJvdJ and AHHB was reached after discussion.

SRS

Twenty-four hours after IV administration of ~ 200 MBq ^{111}In -pentetreotide (Octreoscan; Mallinckrodt, Petten, the Netherlands), planar total-body and 3D single photon emission computed tomography (SPECT) images were obtained.¹⁸ SRS scans were reviewed by a nuclear medicine physician (AHB). In case of discrepancy between the nuclear medicine physician of the referral and research center, a second nuclear medicine physician (KPK) reviewed the SRS, and after discussion between AHB and KPK, consensus was reached.

EUS and ^{11}C -5-HTP PET

If possible, EUS and ^{11}C -5-HTP PET were executed on the same day. EUS was performed with a linear ultrasound endoscope (FG-34UX, Pentax GmbH, Hamburg, Germany) and a scanner system (EUB-525, Hitachi Ultrasound BV, Reeuwijk, the Netherlands). The endoscope had a 60° forward oblique viewing video camera, a 120° scanning ultrasound transducer with a 105° field of view, and a 2.0 mm working channel. The scanning frequency could be switched between 5 and 10 MHz. With power Doppler presence of vascularity was assessed and with elastography imaging,¹⁹ elasticity or rigidity was demonstrated. Patients underwent conscious sedation, and EUS was performed by one endoscopist (HMvD) blinded for other imaging results.

Number and location of pancreatic findings were recorded on a standardized record form. Pancreatic lesions with an-echogenic appearances plus an enhanced ultrasound signal were interpreted as simple cysts. Lesions with a honeycomb pattern were classified as serous microcystic cystadenomas.²⁰ Other focal lesions in the pancreas were considered solid lesions. Fine needle aspiration with a 22 or 25 G needle with a stylet (Sono Tip II 22 or 25 Gauge Medi-Globe GmbH, Germany) was performed on solid lesions if cytological confirmation of pNET was desired by the referred physician. A cytotechnologist was present during the FNA procedure for on-site assessment of the obtained material.

¹¹C-5-HTP PET scans were performed as described previously,¹⁵ either on an ECAT HR+ PET camera (n=11) or on a Siemens Biograph mCT camera (PET/CT 64 slices) (Siemens, Knoxville, TN) (n=11). Maximum standardized uptake value (SUV_{max}) was assessed for each lesion. PET scans were independently and randomly interpreted by two nuclear medicine physicians (AHB, KPK) blinded for all clinical information and other imaging. Number and location of positive lesions were recorded on a standardized record form. In discrepant cases, consensus was reached between AHB and KPK.

The results of the four imaging modalities were discussed in a multidisciplinary team, consisting of a radiologist (EJvdJ), nuclear medicine physician (AHB), gastroenterologist (HMvD), endocrinologist (TPL) and the clinical trial doctor (SJvA). The pancreatic lesions found on both EUS and ¹¹C-5-HTP PET were matched with the CT/MRI+ SRS.

Statistical analysis

A total of 20 patients were estimated to be required to demonstrate additional or new lesions in 25% of the patients with ¹¹C-5-HTP PET and/or EUS. McNemar's test was used for comparison with 80% power and 5% two-sided significance levels.

Analysis was performed at the levels of individual patients and individual lesions. SRS and ¹¹C-5-HTP PET scan are whole body modalities, whereas CT/ MRI cover the abdominal area and EUS the pancreatic region only. Therefore, EUS was compared with other modalities for the pancreatic region only. The percentage of visualized solid lesions was calculated for all four imaging techniques by using a composite reference standard. This standard included the sum of the four imaging outcomes. McNemar's test was used to compare the yield of the four imaging techniques. A *P* value < .05 was considered statistically significant. All authors had access to the study data and had reviewed and approved the final manuscript.

Results

Patient characteristics

Of the 31 eligible patients, 9 declined participation. Patient characteristics of the remaining 22 VHL patients included in this study are presented in Table 1.

Table 1. Patient characteristics (n=22)

Characteristics	Value
Female/Male (n)	12/10
Age in years median/(range)	41/(21-64)
VHL germline mutation (n):	
c.-89-?_c.297+?del	11
c.500G>A	3
c.-213-?_463+?del	2
c.463+2T>C p.(?)	1
c.259_260insA	1
c.497T>C	1
c.509T>A	1
c.241C>T	1
*46,XX.ish del(3)(p25-26p25-26)(cos11-)	1
Earlier pancreatic surgery (n)	
Yes/no	0/22
Abdominal conventional imaging (n)	
MRI	11
CT	11
Serum chromogranin A (µg/L) (n=19)	
Median/range	38/(23-118)
Plasma pancreatic polypeptide (pmol/L) (n=22)	
Median/range	58/(22-234)

Abbreviations: VHL, von Hippel-Lindau; MRI, magnetic resonance imaging; CT, computed tomography.

*According to archaic mutation analysis.

Conventional screening

CT/MRI was positive in 7 patients and detected 9 pancreatic solid lesions. Focal pancreatic uptake on SRS was present in 3 patients, visualizing 3 lesions with increased uptake corresponding with 3 pancreatic solid lesions detected with CT/MRI.

Of the 22 patients, 6 had elevated plasma pancreatic polypeptide with a median of 131 pmol/L (range 115-234 pmol/L). Of the 19 patients evaluable for serum chromogranin A, one had a marginally elevated level of 118 µg/L. In total, 7 patients

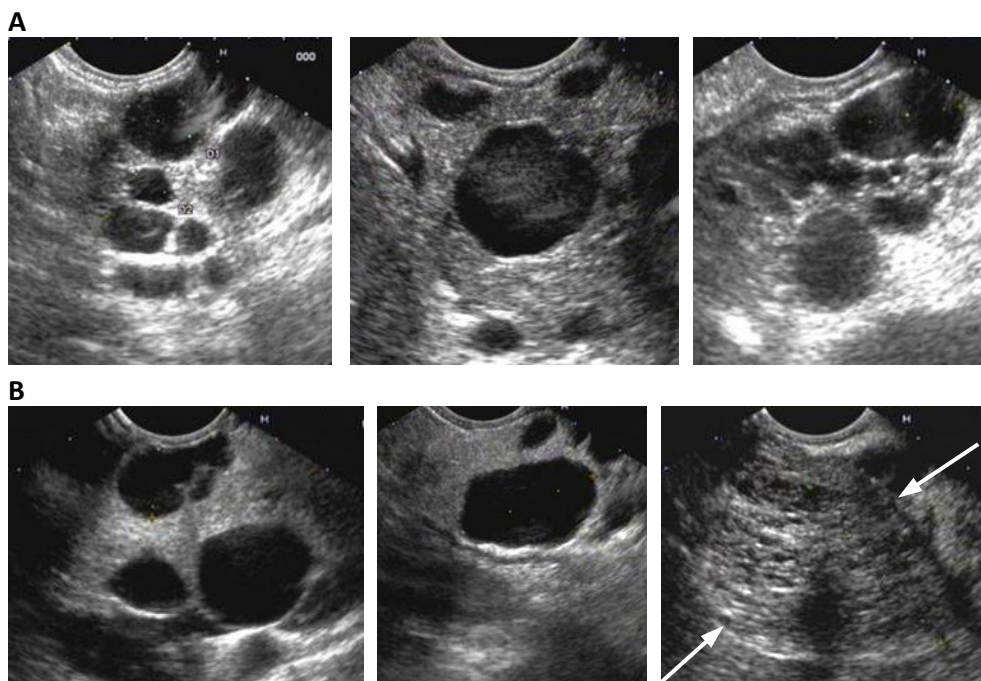


Figure 1. EUS images of pancreatic cysts of two VHL patients. **A** 28 year old man with multiple pancreatic cysts in the entire pancreas, ranging in size from 0.5-1.2 cm. The strongly enhanced ultrasound signal (white regions) is characteristic for cysts. **B** A 36 year old woman with multiple cysts in the entire pancreas and (red arrows) a 4.5 cm microcystic serous cystadenoma with characteristic honeycomb structure in the pancreatic body-tail region.

had elevated tumor markers with 6 not more than a 2-fold elevation. Of these 7 patients, 3 (43%) had pancreatic solid lesions on conventional imaging.

EUS and ^{11}C -5-HTP PET

EUS detected 17 pancreatic solid lesions in 10 patients with a median size of 9.7 mm (range 2.9-55 mm). Most lesions were homogeneous and hypoechoic on EUS with an iso-elastic consistency and hypervascular. In addition, in 18 patients 169 pancreatic cysts were found. See Supplemental Table 1 for EUS characteristics of both cystic and solid lesions.

Only 4 patients had no pancreatic simple cysts or serous microcystic cystadenomas, 12 had 1-10 simple cysts, 4 had > 10 simple cysts, 3 had serous microcystic cystadenoma(s) and 1 patient had almost the complete pancreas replaced by at least 30 cysts. In patients with cysts, the median number of cysts was 4 (range 1-30) per

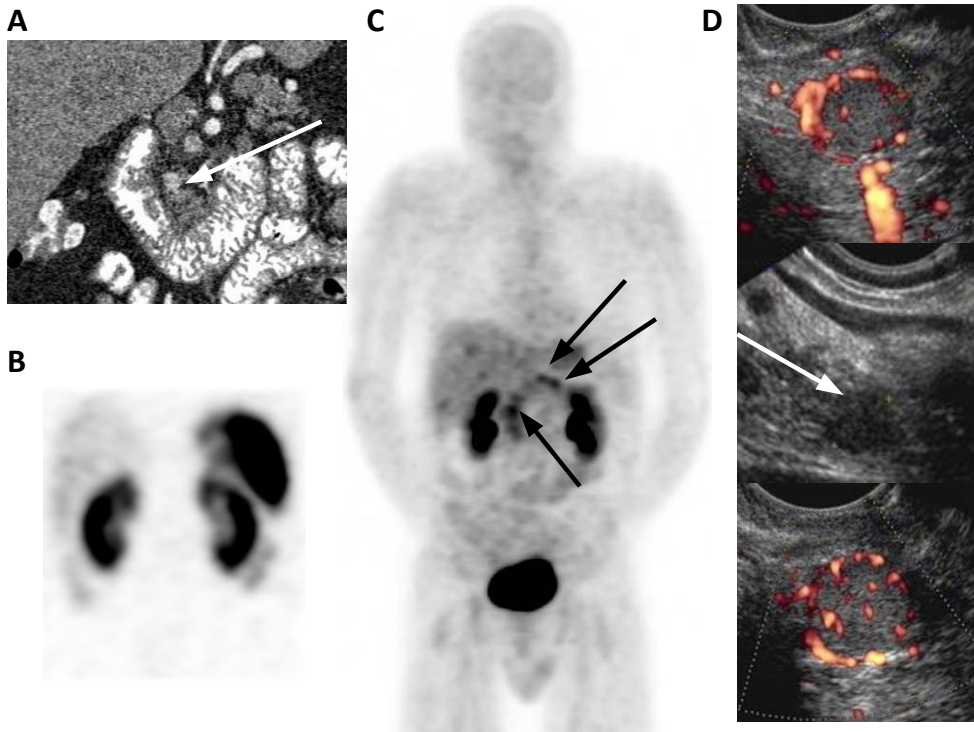


Figure 2. **A** Coronal images of CT scan, **B** SRS SPECT image, **C** maximum intensity projection image of ^{11}C -5-HTP PET and **D** ultrasound images of pancreatic lesions visualized with EUS. In total 4 pancreatic solid lesions were detected. With CT, 1 lesion was found. The SRS was negative. ^{11}C -5-HTP PET detected 3 lesions: 1 in the pancreatic head and 2 in the body-tail region. EUS detected 2 hypoechoic solid lesions in the pancreatic head and 1 in the body-tail region ranging 9.7-14.1 mm. Two solid lesions showed hypervascularity with power Doppler.

patient (Figure 1). In patients with pancreatic solid lesions, the median number of cysts was 1 (range 0-9).

^{11}C -5-HTP PET detected pancreatic lesions in only 1 patient. In this patient 3 pancreatic lesions were visualized with ^{11}C -5-HTP PET with a SUV_{max} ranging from 4.3-4.9. One lesion was confirmed by CT and 2 lesions by EUS (Figure 2).

During the EUS procedure, FNA was performed in 7 solid lesions of 6 patients with a median of 2 passes (range 2-6). The median size was 17 mm (range 7.2-55), of which 3 lesions were < 10 mm. In cell material from 2 lesions of 2 patients, tumor cells were detected. One of these patients was offered for surgery and the other patient remained for follow-up in the VHL surveillance.

In total, 3 patients underwent pancreatic surgery because of large solid lesions suspicious of pNET: the first patient had 1 solid lesion of 5 cm visible on MRI, SRS and EUS, the second patient had 1 lesion of 2 cm visible on MRI, SRS and EUS +

confirmation by cytology, and the third patient had 2 lesions of 4 and 2 cm, both visible on CT and 1 lesion visible on EUS. All 3 patients underwent pylorus preserving pancreaticoduodenectomy. All lesions were hypervascular and inhomogeneous based on EUS. In the first 2 patients histology confirmed the diagnosis of NET. However in the third patient, histology showed that both lesions were serous microcystic cystadenomas.

EUS and ¹¹C-5-HTP PET compared to conventional screening

At a patient-based level, pancreatic solid lesions were found in 10 patients: EUS was positive in 100%, ¹¹C-5-HTP PET in 10%, SRS in 30% and CT/MRI in 70%. At a lesion-based level, 20 pancreatic solid lesions were found with a median size of 9.0 mm (range 2.9-55 mm). EUS detected 17 pancreatic solid lesions, ¹¹C-5-HTP PET 3, CT/MRI 9, SRS 3 and CT/MRI+ SRS found 9. EUS detected the most solid lesions compared to CT/MRI, SRS and CT/MRI+ SRS ($P < .05$) (Table 2). In total, 12 solid lesions were found in the pancreatic head and 8 in the body-tail region, of which EUS detected 11 in the pancreatic head (92%) and 6 in the body-tail region (75%).

Table 2. All patients with pancreatic solid lesions on imaging (n=10)

Imaging modality	n (%) of patients	P value	n (%) of lesions	P value	n (%) of lesions > 1 cm	P value
CT/ MRI	7 (70)	-	9 (45)	-	7 (78)	-
SRS	3 (30)	-	3 (15)	-	3 (38)	-
CT/ MRI+ SRS	7 (70)	-	9 (45)	-	7 (78)	-
¹¹ C-5-HTP PET	1 (10)	* < 0.05	3 (15)	* 0.11	1 (11)	* 0.13
EUS	10 (100)	* 0.25	17 (85)	* < 0.05	8 (89)	* 1

Abbreviations: CT, computed tomography; MRI, magnetic resonance imaging, SRS, somatostatin receptor scintigraphy; ¹¹C-5-HTP PET, ¹¹C-5-hydroxytryptophan positron emission tomography; EUS, endoscopic ultrasound.

*¹¹C-5-HTP PET and EUS, compared with CT/MRI+ SRS.

EUS did not detect 3 solid lesions, and 2 solid lesions were only visualized with CT of which 1 turned out to be a ~3 cm serous cystadenoma at surgery. Another lesion was only visualized with ¹¹C-5-HTP PET.

Of the 9 solid lesions > 1 cm, 8 were detected with EUS, 1 with ¹¹C-5-HTP PET, 7 with CT/MRI, 3 with SRS and 7 with CT/MRI+ SRS (Table 2). Seven patients had pancreatic solid lesions visualized on the conventional imaging techniques CT/MRI+ SRS, in which EUS found 6 additional lesions. ¹¹C-5-HTP PET detected 2 additional lesions in these patients, but missed 8 that were identified with conventional imaging.

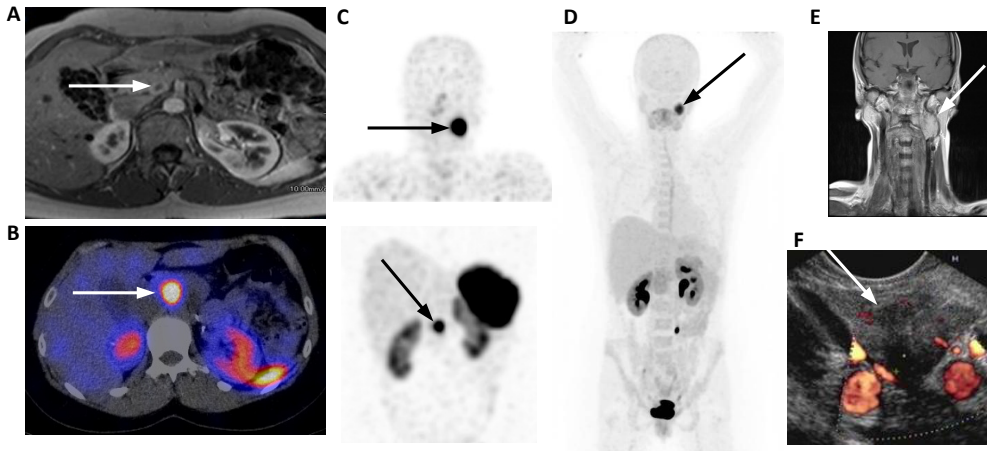


Figure 3. **A** Axial image of abdominal MRI (T1 weighted with contrast), **B** axial image of SRS fused with low-dose CT **C** SRS coronal SPECT image of head and abdominal region, **D** coronal maximum intensity projection of ^{11}C -5-HTP PET, **E** coronal image MRI image of head and neck region and **F** EUS image of the pancreas. On abdominal MRI, 1 pancreatic lesion was found, corresponding with 1 focal lesion on SRS. Moreover on SRS, a focal lesion was visualized in the neck region. ^{11}C -5-HTP PET only showed a lesion in the neck at the same location. MRI of the neck confirmed a paraganglioma. With EUS, the 17 mm pancreatic solid lesion was identified. Cell material obtained by EUS-FNA confirmed the diagnosis of a NET.

However, following resection, 2 of these 8 solid lesions that were ^{11}C -5-HTP PET negative turned out to be serous cystadenomas.

Of the 15 patients without pancreatic solid lesions on CT/MRI plus SRS, none had focal ^{11}C -5-HTP uptake in the pancreas. In 3 of these patients, 4 solid lesions were found with EUS: all were < 1 cm.

Seven patients had elevated tumor markers, of which 3 patients had only pancreatic cysts, 1 patient had multiple cysts and 1 pancreatic solid lesion < 1 cm detected with EUS, 1 patient had 4 pancreatic solid lesions detected with ^{11}C -5-HTP PET, EUS and/or CT, and 2 patients had pancreatic cysts and NETs based on histology.

Extra-pancreatic lesions with nuclear imaging

^{11}C -5-HTP PET detected 15 extra-pancreatic focal lesions in 7 patients (Table 3) (Figure 3). Most lesions corresponded with a hemangioblastoma in the central nervous system (6 lesions in 4 patients) and metastases of an earlier resected renal cell cancer (6 lesions in one patient). Of the 15 ^{11}C -5-HTP PET positive lesions, SRS was positive in 3 lesions of 2 patients. In addition, SRS detected a cerebellar focal lesion

corresponding with a hemangioblastoma on MRI, which was not seen with ^{11}C -5-HTP PET.

Table 3. Extra-pancreatic lesions visualized in seven patients with ^{11}C -5-HTP PET

Patient	Location	SUV _{max}	Diagnosis	Other imaging
A	Neck	15.8	Paraganglioma	MRI, SRS
	Prevertebral	6.4	Paraganglioma, LN	-
B	Kidney (6 lesions)	4.0-10.4	* RCC	[†] CT
C	Eye	3.4	Retinal angioma	Ophthalmoscopy, SRS
	Cerebellum	6.9	Hemangioblastoma	MRI, SRS
D	Cerebellum	#	Hemangioblastoma	MRI
E	Liver	1.3	Serous cystadenoma	CT
F	Cerebellum			
	(2 lesions)	4.3-5.1	Hemangioblastoma	MRI
G	Cerebellum	#	Hemangioblastoma	MRI

Abbreviations: LN, lymph node; RCC, renal cell cancer; MRI, magnetic resonance imaging; SRS, somatostatin receptor scintigraphy; CT, computed tomography

* indicates that diagnosis was histological confirmed

[†] indicates that lesions were visualized retrospectively

SUV_{max} could not be calculated, since uptake was too low for a reliable measurement

Discussion

In this head-to-head comparison of EUS and ^{11}C -5-HTP PET relative to standard pNET screening with CT/MRI and SRS in VHL patients, EUS was superior for pancreatic solid lesion detection. ^{11}C -5-HTP PET had no value in this screening setting. We have shown for the first time that EUS is an excellent method for pancreatic solid lesion detection in VHL disease. EUS can be executed without radiation exposure of the patient, and it allows obtaining cytology for NET confirmation. Therefore, EUS can be of additive value for pancreas imaging in VHL patients.

With EUS we could also identify various lesion characteristics. Most often pancreatic solid lesions were hypoechoic, homogeneous, had an iso-elastic consistency and were hypervascular based on power Doppler. Based on EUS combined with power Doppler, these characteristics might help to identify the characteristics of pNETs. Besides solid lesions, we also detected serous cystadenomas with EUS. Serous cystadenomas of the pancreas include microcystic serous cystadenoma, serous oligocystic and ill-demarcated adenomas as well as macrocystic serous cystadenoma.²⁰

In our series, most cysts were macrocystic serous cystadenomas, recognized by an anechoic appearance. On EUS, 3% of the cysts had a classic honeycomb structure, which is characteristic for serous microcystic cystadenomas. In our study, 2 lesions with a solid appearance on EUS and CT/MRI suspicious of pNET were shown to be serous cystadenomas by means of histology. Overdiagnosis of pNET in VHL has also been reported by others.^{6, 8-9, 12} In our study, one lesion turned out to be a serous cystadenoma, which was clearly hypervascular based on EUS combined with power Doppler. This indicates that a hypervascular nature of pancreatic solid lesions in VHL does not exclude the existence of a serous cystadenomas. Others also reported cases of pancreatic serous cystadenomas having hypervascular appearances on anatomical imaging.²¹⁻²³

To avoid unnecessary surgery, making a distinction between pNET and serous cystadenoma is warranted in VHL disease. EUS potentially allows cytology to be obtained by FNA. However, we obtained adequate material in only 2 out of 7 lesions. This may partly be due to the fact that 3 of the 7 lesions were < 10 mm. In a retrospective study in 15 patients using EUS FNA for confirmation of the diagnosis pNET, the yield was 53%.²⁴ Similar to our series, samples were often hemorrhagic with a low cell yield.²⁴ Other retrospective series reported higher accuracy rates of 90-93%, but it is unclear how patients were selected in these studies.²⁵⁻²⁶ Instead of obtaining cytological material, it is also possible to obtain tissue samples by EUS-guided fine needle tissue acquisition. In a recent prospective study, 30 patients with pancreatic lesions suspected of sporadic pNET underwent fine-needle tissue acquisition with a 19 Gauge needle, without complications.²⁷ In 93% of patients with lesion size ranging from 7 to 100 mm, the NET diagnosis could be confirmed.²⁷ In VHL disease, obtaining tissue samples instead of cell material might also improve the yield.

In general, pNETs have the ability to produce hormones or amines, which provides various options for specific imaging by using this metabolic pathway. In 18 patients with advanced NETs, ¹¹C-5-HTP PET was superior for lesion detection compared to CT.²⁸ In addition, we showed that ¹¹C-5-HTP PET is a more sensitive technique compared to ¹⁸F-DOPA PET and SRS in patients with advanced pNET.¹⁵ Adding CT resulted in a slight improvement of sensitivity.¹⁵ However, in the current VHL study, ¹¹C-5-HTP PET showed no added value for early detection of primary pNETs in VHL patients.

Besides pancreatic lesions, ¹¹C-5-HTP PET found 15 other VHL manifestations, including hemangioblastomas, renal cell carcinomas and paraganglioma. Like pNETs, paragangliomas are able to take up and decarboxylate amine precursors.²⁹ This

property has not been identified in renal cell carcinomas and hemangioblastomas. Nevertheless, in both tumor types immunohistochemical studies showed positivity for specific neuroendocrine markers, including neuron specific enolase and synaptophysin,^{30,31} indicating presence of neuroendocrine properties of these cells. This might clarify visualization with ¹¹C-5-HTP PET.

The presence of somatostatin receptor subtype 2 on NET cells is essential for tumor imaging with SRS.³² In our study, the value of SRS was limited, since only 15% of pancreatic solid lesions could be visualized. Another study showed a SRS patient-based positivity of 59% in 27 VHL patients with pNETs with a median size of 30 mm (range 10-80 mm).³³ An explanation for the lower yield of SRS in our study could be that the median size of the solid pancreatic lesions was ~3-fold smaller compared to the study of Corcos et al.³³ Altogether, this suggests that SRS is not useful for pNET screening in VHL disease.

In our series, 2 out of 4 patients with a cytologically/histologically confirmed NET had elevated serum chromogranin A or plasma pancreatic polypeptide levels. In total, 7 patients had elevated tumor markers, which were marginally increased in 6 patients (not more than 2 times the upper limit of normal). The biological and analytical variations of these markers are not known, making it difficult to interpret these findings. Moreover, false-positive values can occur in a variety of clinical conditions. Elevated chromogranin A levels can occur due to use of proton pump inhibitors, renal or hepatic insufficiency, and elevated pancreatic polypeptide levels due to high age, diarrhea or gut inflammation.^{16, 34} In a large series of 108 VHL patients with pNETs in which the serum tumor markers insulin, glucagon, pancreatic polypeptide and vasoactive intestinal peptide were evaluated, none were indicative for pNET in VHL.⁸ This indicates that measurement of these tumor markers is likely of no value.

The current available VHL guidelines recommend for adults yearly abdominal imaging by CT⁶ or yearly transabdominal ultrasound and MRI at least every other year.¹⁰ However, the sensitivity of transabdominal ultrasound is low and CT has the disadvantages of radiation exposure and use of iodine-containing contrast. MRI does not include radiation exposure, but requires gadolinium-containing contrast, which can be nephrotoxic.³⁵ Therefore, transabdominal ultrasound combined with EUS might replace them. The invasive character of EUS is a disadvantage by both clinicians and patients. However in general EUS in combination with conscious sedation is well tolerated.³⁶

Our findings illustrate that EUS is of additional value in VHL patients for early pancreatic solid lesion detection. Apart from its high sensitivity, EUS can be combined with FNA to obtain cytology for NET confirmation. EUS may moreover identify

different lesion characteristics, it is in general a well-tolerated procedure and it can be executed without radiation exposure and use of contrast agents. Therefore, we suggest to use EUS in the surveillance of VHL disease.

Acknowledgments We would like to thank Drs DJ. Gouma and D. O'Toole for their contributions as members of the external monitoring committee.

Funding Supported by a Grant of the Dutch Cancer Society (RUG 2008-4188).

References

1. Yao JC, Eisner MP, Leary C, et al. Population-based study of islet cell carcinoma. *Ann Surg Oncol* 2007;14:3492-3500.
2. Zhou J, Enewold L, Stojadinovic A, et al. Incidence rates of exocrine and endocrine pancreatic cancers in the United States. *Cancer Causes Control* 2010;21:853-861.
3. Latif F, Tory K, Gnarr J, et al. Identification of the von Hippel-Lindau disease tumor suppressor gene. *Science* 1993;260:1317-1320.
4. Maher ER, Iselius L, Yates JR, et al. Von Hippel-Lindau disease: a genetic study. *J Med Genet* 1991;28:443-447.
5. Wilding A, Ingham SL, Laloo F, et al. Life expectancy in hereditary cancer predisposing diseases: an observational study. *J Med Genet* 2012;49:264-269.
6. Lonser RR, Glenn GM, Walther M, et al. Von Hippel-Lindau disease. *Lancet* 2003;361:2059-2067.
7. Hammel PR, Vilgrain V, Terris B, et al. Pancreatic involvement in von Hippel-Lindau disease. *The Groupe Francophone d'Etude de la Maladie de von Hippel-Lindau. Gastroenterology* 2000;119:1087-1095.
8. Blansfield JA, Choyke L, Morita SY, et al. Clinical, genetic and radiographic analysis of 108 patients with von Hippel-Lindau disease (VHL) manifested by pancreatic neuroendocrine neoplasms (PNETs). *Surgery* 2007;142:814-818.
9. Neuzillet C, Vullierme MP, Coulevar A, et al. Difficult diagnosis of atypical cystic pancreatic lesions in von Hippel-Lindau disease. *J Comput Assist Tomogr* 2010;34:140-145.
10. The VHL handbook (<http://www.vhl.org/handbook/vhlhb4.php#Suggested>) (access date: 10 January 2013).
11. http://www.nccn.org/professionals/physician_gls/pdf/neuroendocrine.pdf (access date: 10 January 2013).
12. Kitano M, Millo C, Rahbari R, et al. Comparison of 6-18F-fluoro-L-DOPA, 18F-2-deoxy-D-glucose, CT and MRI in patients with pancreatic neuroendocrine neoplasms with von Hippel-Lindau disease. *Surgery* 2011;150:1122-1128.
13. Rösch T, Lightdale CJ, Botet JF, et al. Localization of pancreatic endocrine tumors by endoscopic ultrasonography. *N Engl J Med* 1992;326:1721-1726.
14. Sundin A, Eriksson B, Bergström M, et al. Demonstration of [11C]-5-hydroxy-L-tryptophan uptake and decarboxylation in carcinoid tumors by specific positioning labeling in positron emission tomography. *Nucl Med Biol* 2000;27:33-41.
15. Koopmans KP, Neels OC, Kema IP, et al. Improved staging of patients with carcinoid and islet cell tumors with 18F-dihydroxy-phenyl-alanine and 11C-5-hydroxy-tryptophan positron emission tomography. *J Clin Oncol* 2008;26:1489-1495.
16. Modlin IM, Gustafsson BI, Moss SF, et al. Chromogranin A—Biological function and clinical utility in neuroendocrine tumor disease. *Ann Surg Oncol* 2010;17:2427-2443.
17. Reznik RH. CT/MRI of neuroendocrine tumours. *Cancer imaging* 2006;S163-S177.

18. Balon HR, Goldsmith SJ, Siegel BA, et al; Society of Nuclear Medicine. Procedure guideline for somatostatin receptor scintigraphy with (111)In-pentetreotide. *J Nucl Med* 2001;42:1134-1138.
19. Iglesias-Garcia J, Larino-Noia J, Abdulkader I, et al. EUS elastography for the characterization of solid pancreatic masses. *Gastrointest Endosc* 2009;70:1101-1108.
20. Compton CC. Serous cystic tumors of the pancreas. *Semin Diagn Pathol* 2000;17:43-55.
21. Gabata T, Terayama N, Yamashiro M, et al. Solid serous cystadenoma of the pancreas: MR imaging with pathologic correlation. *Abdom Imaging* 2005;30:605-609.
22. Takeshita K, Kutomi K, Takada K, et al. Unusual imaging appearances of pancreatic serous cystadenoma: correlation with surgery and pathologic analysis. *Abdom Imaging* 2005;30:610-615.
23. Gerke H, Silva R, Jensen CS. Hypervascular pancreatic tumor diagnosed as a serous cystadenoma by EUS-guided Trucut biopsy. *Gastrointest Endosc* 2006;64:273-274.
24. Voss M, Hammel P, Molas G, et al. Value of endoscopic ultrasound guided fine needle aspiration biopsy in the diagnosis of solid pancreatic masses. *Gut* 2000;46:244-249.
25. Ardengh JC, de Paulo GA, Ferrari AP. EUS-guided FNA in the diagnosis of pancreatic neuroendocrine tumors before surgery. *Gastrointest Endosc* 2004;60:378-384.
26. Figueiredo FA, Giovannini M, Monges G, et al. Pancreatic endocrine tumors: a large single-center experience. *Pancreas* 2009;38:936-940.
27. Larghi A, Capurso G, Garnuccio A, et al. Ki-67 grading of nonfunctioning pancreatic neuroendocrine tumors on histologic samples obtained by EUS-guided fine-needle tissue acquisition: a prospective study. *Gastrointest Endosc* 2012;76:570-577.
28. Orlefors H, Sundin A, Ahlström H, et al. Positron emission tomography with 5-hydroxytryptophan in neuroendocrine tumors. *J Clin Oncol* 1998;16:2534-2541.
29. Eisenhofer G. Screening for pheochromocytomas and paragangliomas. *Curr Hypertens Rep* 2012;14:130-137.
30. Becker I, Paulus W, Roggendorf W. Histogenesis of stromal cells in cerebellar hemangioblastomas. *Am J Pathol* 1989;134:271-275.
31. Ronkainen H, Soini Y, Vaarala MH, et al. Evaluation of neuroendocrine markers in renal cell carcinoma. *Diagn Pathol* 2010;5:28.
32. Teunissen JJ, Kwekkeboom DJ, Valkema R, et al. Nuclear medicine techniques for the imaging and treatment of neuroendocrine tumours. *Endocr Relat Cancer* 2011;18:S27-S51.
33. Corcos O, Coulevard A, Giraud S, et al. Endocrine pancreatic tumors in von Hippel-Lindau disease: clinical, histological and genetic features. *Pancreas* 2008;37:85-93.
34. Oberg K. Circulating biomarkers in gastroenteropancreatic neuroendocrine tumours. *Endocr Relat Cancer* 2011;18:S17-S25.
35. Perazella MA. Current status of gadolinium toxicity in patients with kidney disease. *Clin J Am Soc Nephrol* 2009;4:461-469.
36. Bonta PI, Kok MF, Bergman JJ, et al. Conscious sedation for EUS of the esophagus and stomach: a double-blind, randomized, controlled trial comparing midazolam with placebo. *Gastrointest Endosc* 2003;57:842-847.

Supplemental Table 1. EUS characteristics of pancreatic solid lesions (n=17) and cysts (n=139)

Characteristics	Solid lesions (n)	Cystic lesions (n)
Localization:		
Pancreatic head	11	56
Pancreatic body-tail	6	83
Lesion size		
> 1 cm	7	47
≤ 1 cm	10	92
Relation pancreatic duct		
Yes	6	5
No	11	74
Unknown	0	60
Echogenic pattern		
Hyperechoic	0	0
Hypoechoic	17	0
Anechoic	0	139
Ultrasonographic texture		
Homogeneous	11	133
Heterogeneous	6	6
Power Doppler signal		
Positive	10	*
Negative	7	*
Elastography		
Rigid	2	*
Iso-elastic	11	*
Unknown	4	*
Honeycomb structure		
Yes	*	4
No	*	135

*Indicates that characteristic is not applicable

Note that the patient in which almost the total pancreas was replaced by cysts, has not been evaluated for cystic lesion characteristics.